

Micromorphology of an Early Holocene Loess-Paleosol Sequence, Central Alaska, U.S.A

Author: Josephs, Richard L.

Source: Arctic, Antarctic, and Alpine Research, 42(1) : 67-75

Published By: Institute of Arctic and Alpine Research (INSTAAR),
University of Colorado

URL: <https://doi.org/10.1657/1938-4246-42.1.67>

BioOne Complete (complete.BioOne.org) is a full-text database of 200 subscribed and open-access titles in the biological, ecological, and environmental sciences published by nonprofit societies, associations, museums, institutions, and presses.

Your use of this PDF, the BioOne Complete website, and all posted and associated content indicates your acceptance of BioOne's Terms of Use, available at www.bioone.org/terms-of-use.

Usage of BioOne Complete content is strictly limited to personal, educational, and non - commercial use. Commercial inquiries or rights and permissions requests should be directed to the individual publisher as copyright holder.

BioOne sees sustainable scholarly publishing as an inherently collaborative enterprise connecting authors, nonprofit publishers, academic institutions, research libraries, and research funders in the common goal of maximizing access to critical research.

Micromorphology of an Early Holocene Loess-Paleosol Sequence, Central Alaska, U.S.A.

Richard L. Josephs*

*Department of Geoscience, University of Iowa, Iowa City, Iowa 52242, U.S.A.
richard-josephs@uiowa.edu

Abstract

This paper describes a micromorphological investigation of an early Holocene loess-paleosol sequence at the Chena Hot Springs Road site, a highway road cut exposure near Fairbanks, Alaska, U.S.A. The procedure identified and described soil microstructure, basic mineral components and their related distributions, organic inclusions, and pedogenic features. Micromorphology confirmed the presence of a number of thin, discontinuous, weakly expressed soils that evince disturbance by diagenetic, graviturbative, and cryoturbative processes. Well-preserved organic remains indicate the presence of a boreal forest that would have acted as a highly effective sediment trap. The frequent observation of detrital iron-oxide grains is consistent with other studies of area loess that reveal high concentrations of magnetite and ilmenite, resulting in significant increases in magnetic susceptibility. Increases in wind strength are likely responsible for the increased clay content in the buried paleosols. Loess deposition, which would inhibit pedogenesis, is probably related to greater wind strength, while pedogenesis, indicative of stability and minimal deposition, suggests periods of reduced wind.

DOI: 10.1657/1938-4246-42.1.67

Introduction

The value of loess as a paleoclimate proxy has been documented in many parts of the world (Kukla et al., 1988; Hovan et al., 1989; Maher and Thompson, 1992; Verosub et al., 1993; Xiao et al., 1995; Kemp and Derbyshire, 1998; Liu and Ding, 1998; Kemp, 1999; Muhs and Zárate, 2001; Bettis et al., 2003; Kemp et al., 2006; Sanborn et al., 2006; Stevens et al., 2007). Alaskan loess is of particular interest for paleoclimate studies because it is one of the most extensive and best studied high-latitude loess sequences in the world. Holocene loess records as complete and extensive as those contained in Alaskan loess are rare (Péwé, 1975; Begét, 1990, 2001; Vlag et al., 1999; McDowell and Edwards, 2001; Muhs et al., 2001, 2003, 2008; Lagroix and Banerjee, 2002). Westgate et al. (1990) suggested that the Alaskan loess record may extend as far back as three million years.

Recent studies document the existence of numerous buried soils within loess deposits across central Alaska and the Canadian Yukon (Hamilton et al., 1988; Begét and Hawkins, 1989; Begét, 1990; Begét et al., 1990; Hamilton and Brigham-Grette, 1991; Vlag et al., 1999; McDowell and Edwards, 2001; Muhs et al., 2001, 2003, 2008; Lagroix and Banerjee, 2002; Sanborn et al., 2006). Their presence indicates periods of relative landscape stability when loess deposition rates were significantly reduced so that pedogenesis could occur (Muhs and Bettis, 2003; Muhs et al., 2003, 2008).

Morphological and chemical properties of buried soils can provide a wealth of information about past environmental conditions. In addition to being an indicator of landscape stability, paleosols can also be used: (1) to provide information about paleotopography, (2) as stratigraphic markers, and (3) to reconstruct the paleoclimate and the paleovegetation under which they formed (Wright, 1986; Birkeland, 1999; Kemp, 1999; Muhs et al., 2001, 2003, 2008; Josephs and Spiess, 2004; Josephs and

Rankin, 2008). This study uses micromorphology—the study of intact, oriented samples of soil and sediment in thin section—to investigate the alternating early Holocene interglacial cycles of loess deposition and pedogenesis evinced at the Chena Hot Springs Road site, a highway road cut exposure approximately 16 km east-northeast of the City of Fairbanks, Alaska, U.S.A. (Fig. 1). Micromorphology was incorporated into the overall research strategy at the Chena Hot Springs Road site because of its documented success in elucidating paleoenvironmental change from pedosedimentary (microstratigraphic and microstructural) features (Dumanski and St. Arnaud, 1966; Van Vliet-Lanoë, 1985, 1998; Bronger and Heinkele, 1989; Fedoroff et al., 1990; Kemp and Derbyshire, 1998; Kemp, 1999; Todisco and Bhiry, 2008).

Physical Setting and Stratigraphy

The Chena Hot Springs Road site is located within the Tanana River valley and is bordered by the Yukon-Tanana Upland to the north and east and by the Alaska Range to the south (Fig. 1). The area's predominant bedrock is Precambrian to lower Paleozoic Fairbanks Schist—a highly deformed, strongly jointed, quartz-mica and quartzite schist (Fig. 2) (Robinson et al., 1990). With the exception of a few small valley glaciers in the Yukon-Tanana Upland, the Fairbanks area was never glaciated (Péwé et al., 1967). In the Alaska Range to the south, large glaciers are present and were present to a greater extent during the last glacial period (Hamilton, 1994).

Loess is widespread across central Alaska; however, the exact source of the deposits is uncertain. The most likely sources for Fairbanks-area loess are the local bedrock (the Fairbanks Schist), fluvial deposits of the Yukon River to the north, and fluvial deposits of the Tanana and Nenana rivers to the south (Muhs and Budahn, 2006). On the higher ridges bordering the Tanana River

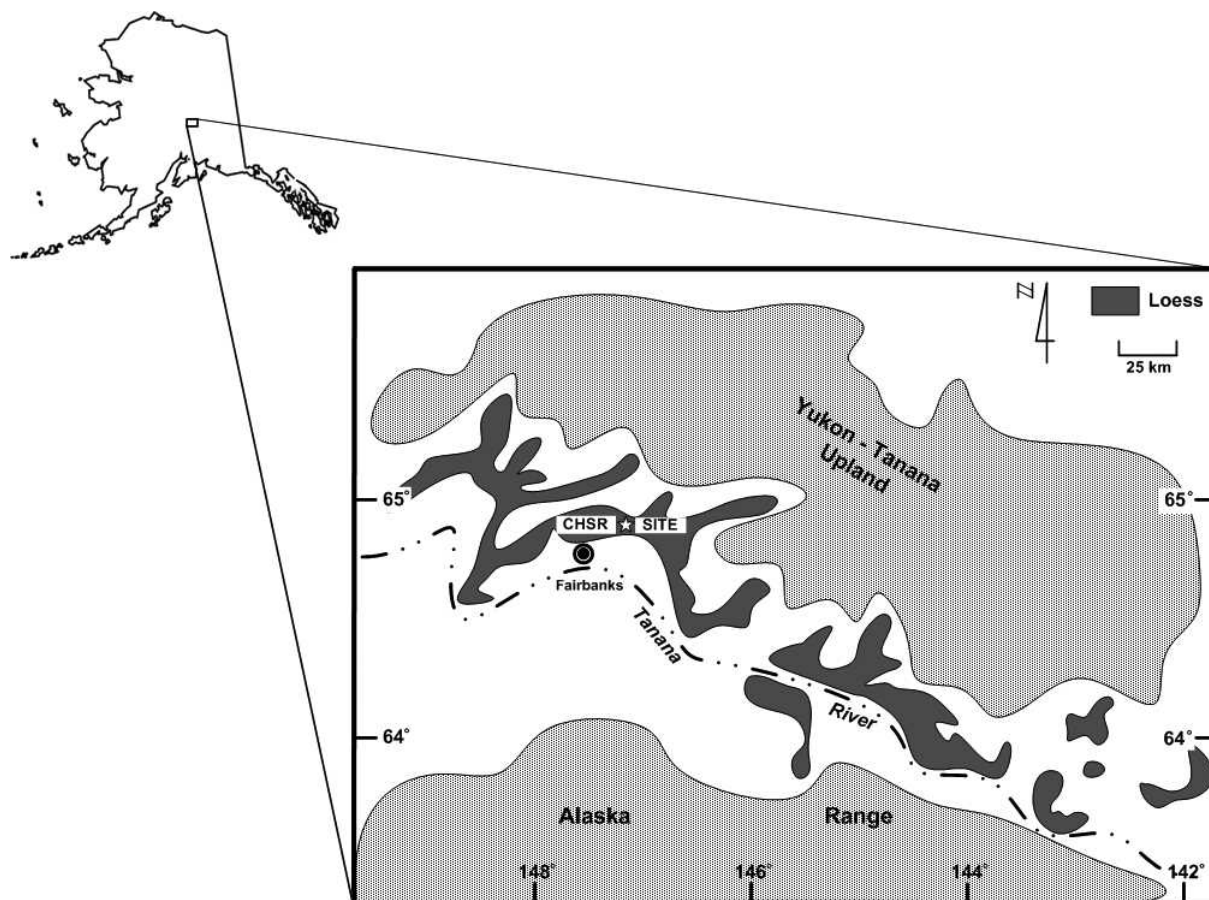


FIGURE 1. Chena Hot Springs Road (CHSR) site location map showing the distribution of loess within the Tanana River valley (modified from Muhs et al., 2003).

valley, the loess is about 30 cm thick; on the lower elevations nearer the river, it can be as much as 60 m thick (Péwé et al., 1966). The Chena Hot Springs Road site is an upland setting that received direct air-fall loess (Péwé et al., 1966; Muhs et al., 2003). Here, the loess is draped over an upland bedrock ridge crest. It is thinnest across the ridge crest and gradually thickens downslope. Loess deposition has been active across central Alaska since before the last interglacial period and has continued into the Holocene (Muhs et al., 2003).

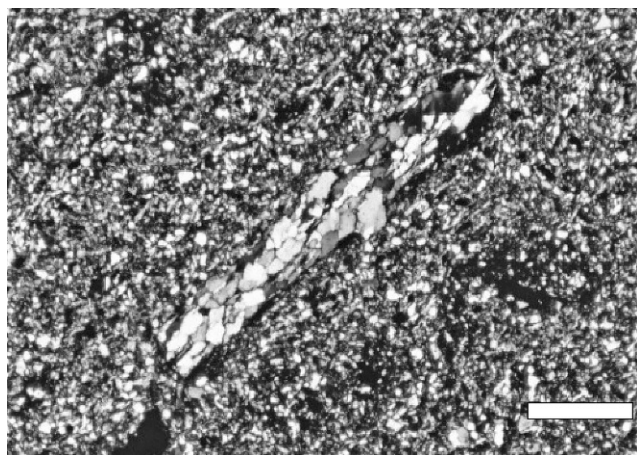


FIGURE 2. Photomicrograph (XPL @ 20X) from sample 4 of 2-mm-long quartz-mica schist fragment (scale bar = 0.5 mm).

The Fairbanks silt loam—a coarse-silty, mixed, superactive Typic Haplocryept with an O/E/Bw/C profile—is the mapped soil unit at the Chena Hot Springs Road site (White et al., 2002; Mulligan, 2004). Soils of the Fairbanks Series are very deep (>150 cm thick), well-drained, strongly acid (surface soil) to neutral (subsoil) soils that exhibit moderate permeability. They typically contain between 2 and 6% organic matter. The parent material is micaceous loess (White et al., 2002; Mulligan, 2004).

The Fairbanks silt loam occurs on mountain backslopes and south-facing hills with slopes ranging between 12 and 20%. Permafrost is not present on moderately to steeply sloping south-facing hillsides; however, this soil does experience seasonal cryoturbation, which can effectively obliterate soil horizon boundaries and even invert soil horizons (White et al., 2002; Mulligan, 2004; Muhs et al., 2008). Fairbanks Series' soils typically form under boreal forest dominated by white spruce (*Picea glauca*), paper birch (*Betula papyrifera*), and quaking aspen (*Populus tremuloides*) (White et al., 2002; Mulligan, 2004).

Buried soils are common in the Fairbanks area (Muhs et al., 2003, 2008). They indicate periods of landscape stability when loess deposition either temporarily ceased, or decreased sufficiently enough, so that pedogenesis could effectively operate (Muhs et al., 2003). Muhs et al. (2008) summarized the use of soil color to identify buried soils within Fairbanks area loess-paleosol sequences. They stated that unaltered loess typically has a light brownish gray (2.5Y 6/2), light yellowish brown (2.5Y 6/3), or grayish brown (2.5Y 5/2) color, whereas soil O or A horizons have 10YR or 7.5YR hues and much lower values and chromas. Soil B horizons,

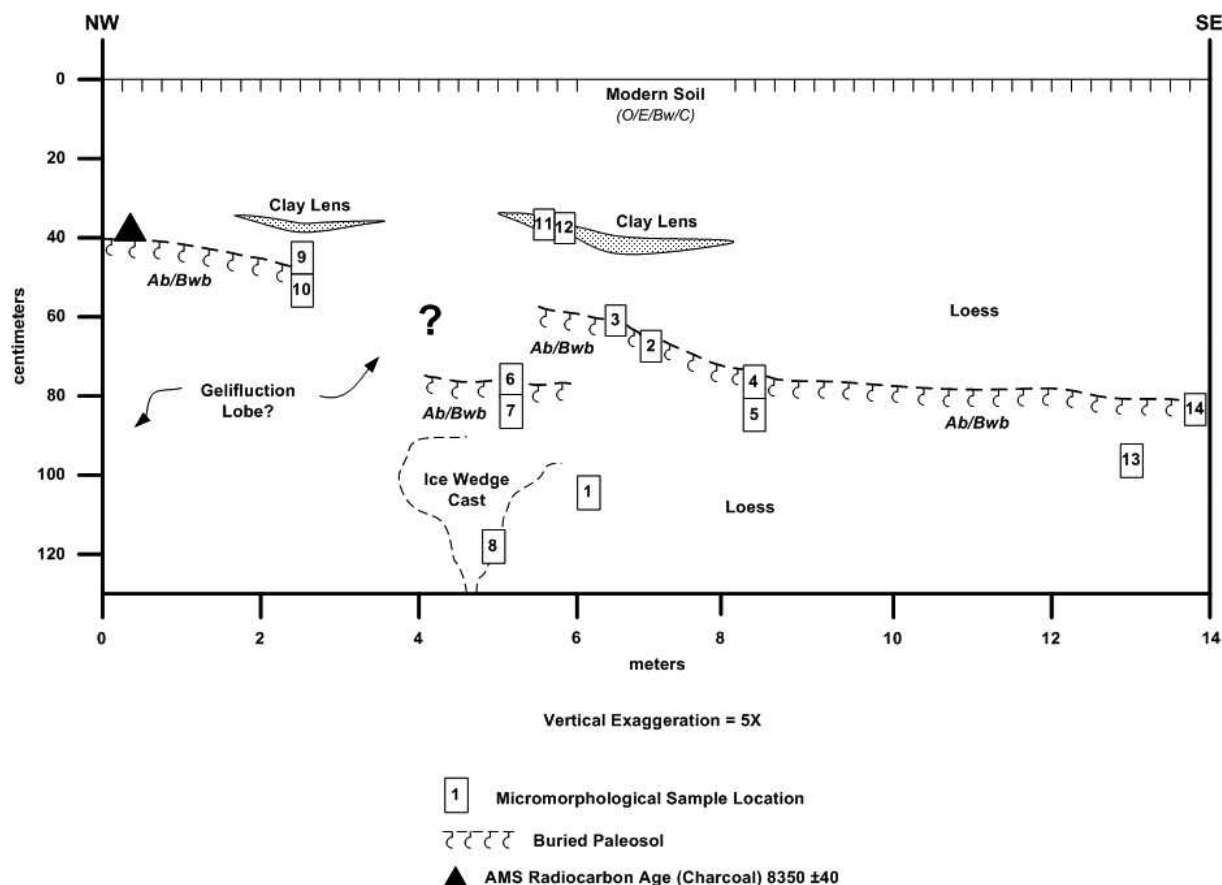


FIGURE 3. Profile of the easternmost section of the northerly road cut exposure, Chena Hot Springs Road, showing the micromorphological sample locations, paleosol horizon, and subsurface features.

where present, also have 10YR or 7.5YR hues with chromas that are much higher than unaltered loess. Organic matter and fine silt and clay content are also generally higher in the paleosols.

Methods

A total of 14 thin sections were prepared from samples collected at the eastern end of a south-facing road cut exposure (Fig. 3), along the northerly right-of-way of the Chena Hot Springs Road, using a sampling method outlined in Josephs and Bettis (2003). A profile map, plotting the locations of the soil horizons, subsurface features, and sample boxes, was compiled in the field by the author and Dr. Arthur Bettis, Department of Geoscience, University of Iowa.

The 14 samples were collected from the buried, early Holocene paleosol, the underlying loess, and across the boundary of an ice wedge cast. The samples were prepared by Spectrum Petrographics, Inc., Vancouver, Washington, U.S.A. They were vacuum-impregnated with a clear, epoxy-based resin, trimmed and bonded to a glass microscope slide measuring 75 × 50 mm, and ground to a final thickness of 30 microns (0.03 mm), rendering them translucent. The resulting thin sections were examined with a Nikon Optiphot-Pol polarizing microscope. The procedure allows identification and description of soil/sediment microstructure, basic mineral components and their related sizes and distributions, organic inclusions, and features resulting from various soil-forming processes (pedofeatures). The descriptions follow the terminology of Bullock et al. (1985) and Stoops (2003) (Table 1). Following standard convention, all of the photomicrographs presented in this article (Figs. 2, 4, 5, 6 [A–D], 7, 8, and 9) are

oriented so that the original ground surface (the “up” direction) is toward the top of the image.

Results

The 14 micromorphological samples examined in this study date between 10,000 and 8000 ^{14}C yr B.P. (Muhs et al., 2003). As part of a previous investigation, an Accelerator Mass Spectrometric (AMS) radiocarbon age of 8350 ± 40 (WW-3181) was obtained from a piece of charcoal collected 40 cm below the

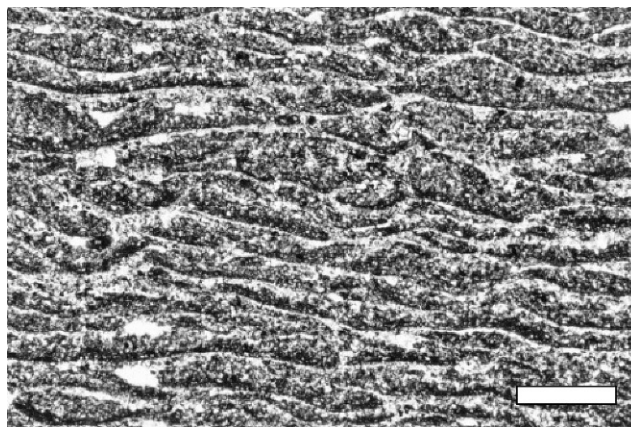


FIGURE 4. Photomicrograph (PPL @ 20×) from sample 10, displaying lenticular platy microstructure in the buried paleosol (scale bar = 0.5 mm).

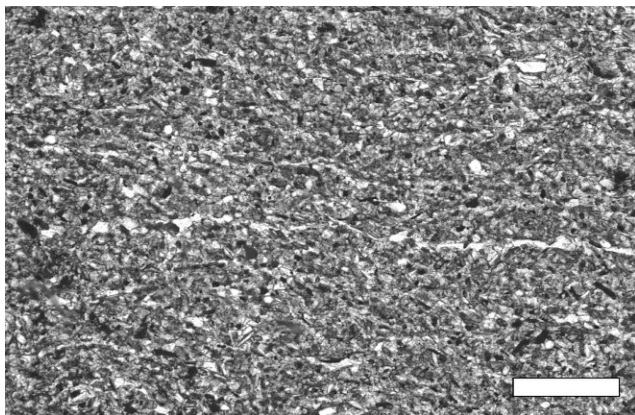


FIGURE 5. Photomicrograph (PPL @ 20×) from sample 1, displaying compact grain microstructure with a platy overprint, developed in loess underlying the buried paleosol (scale bar = 0.5 mm).

surface at this easternmost end of the road cut exposure (Fig. 3) (Muhs et al., 2003: Table 1 [p. 195] and Fig. 12 [p. 1963]).

Although described as a very deep soil (>150 cm [White et al., 2002; Mulligan, 2004]), the modern soil developed at the study site is only between 40 and 80 cm thick with an O/E/Bw/C profile. The uppermost, early Holocene paleosol has a highly compacted Ab/Bwb profile that dips northwest to southeast between roughly 40 and 80 cm below the existing ground surface (Fig. 3). There is an approximate 3-m-wide gap in the western half of the profile where the buried soil is absent. A section of the missing paleosol is present 20 to 25 cm below this gap. The break appears to result from the downslope (west to east) movement of a gelifluction lobe (Fig. 3).

MICROSTRUCTURE AND COMPOSITION

The majority of the thin sections display distinct platy microstructure (Fig. 4), and all are composed of unoriented, well-sorted, angular to subangular, silt-sized quartz and mica, primarily muscovite, in a single-spaced to close porphyric coarse/fine related distribution pattern (c/f RDP) (Bullock et al., 1985; Stoops, 2003). The percentage of feldspar minerals is very low, and, of those few observed, plagioclase is the more common variety. Péwé (1955) and Muhs et al. (2003, 2008) also identified these as the major minerals in Fairbanks-area loesses. No evidence of carbonate mineralization was observed, which is also consistent with the results of previous geochemical analyses (Muhs et al., 2003, 2008).

Platy microstructure (banded cryogenic fabric or isoband cryogenic fabric) is common in soils and sediments that experience repeated freeze-thaw cycles (Dumanski and St. Arnaud, 1966; Van Vliet-Lanoë, 1985; Kemp, 1999; Todisco and Bhiry, 2008). It is formed by ice lensing—a cryogenic process that produces predominantly horizontal, micro- to macroscopic, lens-shaped bodies of ice that grow parallel to the thermal gradient of the soil or sediment (Van Vliet-Lanoë, 1985, 1998). When a soil is subjected to numerous freeze-thaw cycles, erosion and plastic deformation of the groundmass caused by ice lensing results in a “lenticular” platy microstructure (Fig. 4) (Van Vliet-Lanoë, 1985; Kemp 1999; Mason et al., 2007; Sanborn et al., 2006; Todisco and Bhiry, 2008). The platy microstructure is most strongly expressed in those samples that were collected high up in the profile. Some of the deepest recovered samples (e.g., 1, 5, and 13; Figs. 3 and 5) display more of a compact grain microstructure with a platy

overprint. This is likely the result of greater compaction that acts to mitigate the cryogenic effects. The micromass displays a stipple-speckled birefringence fabric (b-fabric) produced by randomly oriented fine silt- and clay-sized particles (Bullock et al., 1985; Stoops, 2003). Previous investigations have identified smectite, Mg-rich chlorite, mica, and kaolinite as the predominant clay minerals in central Alaskan loess (Muhs et al., 2003).

ORGANIC MATTER

All 14 thin sections contain varying amounts of organic material in the form of plant residues, excrements (fecal pellets), and pedogenically derived organic coatings (organans) and concentrations (Brewer, 1976; Bullock et al., 1985; Stoops, 2003). The overall state of preservation of the included plant remains in both the loess and paleosol horizons is quite good, and the majority display morphology that is consistent with boreal forest species (Fig. 6).

The evidence for boreal forest species is important because the amount and type of vegetation present on the landscape is the critical factor favoring loess-trapping efficiency (Tsoar and Pye, 1987; Muhs et al., 2001, 2003). During the last glacial period, tundra was the dominant vegetation in the Fairbanks area and much of central Alaska. Boreal forests re-entered central Alaska between 8000 and 9000 ¹⁴C yr B.P. (Ager, 1983; Ager and Brubaker, 1985). Muhs et al. (2001, 2003) proposed that the greater dust-trapping efficiency of boreal forests explains increased loess accumulation in the Holocene, because detailed mapping of loess thickness and distribution demonstrates that most loess occurs in areas covered by boreal forest. Tsoar and Pye (1987, p. 147) determined that “forest is more efficient in trapping dust than steppe or tundra vegetation due to its greater roughness.”

DETRITAL IRON-OXIDE MINERAL GRAINS

Due to their opacity, it proved difficult to distinguish, and accurately quantify, iron-oxide mineral grains (opaques) from isolated pieces of organic matter and organically coated grains. It was determined that the iron-oxide grains could be better distinguished from the organic matter and organically coated mineral grains using reflected light rather than polarized light. In reflected light, the metallic properties of the iron-oxide grains produce a dark-bluish to black tint, whereas the less dense, non-metallic organic matter and coatings fade to dark browns, dark yellowish browns, and orange browns, often with translucent edges. The surface area of opaque grains is also more accurately represented in reflected light (i.e., the Holmes Effect) (Chayes, 1956). Iron-oxide grains were identified in all 14 thin sections (Fig. 7).

Problems associated with the identification of the iron-oxide grains precluded an accurate quantitative assessment of their concentrations with respect to the unaltered loess and the paleosols. Previous geochemical analyses found an unusually high bulk Fe₂O₃ content in central Alaskan loess (Muhs et al., 2003). Magnetite (Fe₃O₄) and ilmenite (FeTiO₃) have been identified as the primary opaque minerals in upland loess within the Fairbanks area (Péwé, 1955). Loess deposits within central Alaskan loess-paleosol sequences exhibit greater magnetic susceptibility relative to the buried paleosols, indicating stronger wind conditions capable of transporting heavier, more magnetic (iron-bearing) particles during periods of loess accumulation (Begét et al., 1990).

TABLE 1
Micromorphological descriptions (terminology based on Bullock et al. [1985] and Stoops [2003]).

Sample ID	Description	Microstructure	c/f Related Distribution Pattern	Coarse Fraction	Micromass (b-fabric)	Voids	Pedofeatures	Organic Material
1	loess below paleosol	compact grain with platy overprint	single-spaced to close porphyric	quartz, K-feldspar, plagioclase feldspar, muscovite, opaques	stipple-speckled with minor undifferentiated	planes, vughs	coatings, nodules, infillings	plant residues
2	across buried A/Bw horizons	platy	single-spaced to close porphyric	quartz, K-feldspar, plagioclase feldspar, muscovite, opaques	stipple-speckled with minor undifferentiated	planes, vughs	coatings, nodules, infillings	plant residues
3	across buried A/Bw horizons	platy	single-spaced to close porphyric	quartz, K-feldspar, plagioclase feldspar, muscovite, opaques	stipple-speckled with minor undifferentiated	planes, vughs	coatings, nodules, infillings	plant residues
4	across buried A/Bw horizons	compact grain with platy overprint to platy in upper portion, subangular blocky at bottom	single-spaced to close porphyric	quartz, K-feldspar, plagioclase feldspar, muscovite, opaques	stipple-speckled with minor undifferentiated, granostratified in lower (clay) portion	planes, vughs	coatings, nodules, infillings	plant residues
5	loess below paleosol	compact grain with platy overprint	single-spaced to close porphyric	quartz, K-feldspar, plagioclase feldspar, muscovite, opaques	stipple-speckled with minor undifferentiated	planes, vughs	coatings, nodules, infillings, excrements	plant residues
6	loess and upper portion of buried A/Bw-horizons	platy	single-spaced to close porphyric	quartz, K-feldspar, plagioclase feldspar, muscovite, opaques	stipple-speckled with minor undifferentiated	planes, vughs	coatings, nodules, infillings, excrements	plant residues
7	lower portion of buried A/Bw horizons	platy	single-spaced to close porphyric	quartz, K-feldspar, plagioclase feldspar, muscovite, opaques	stipple-speckled with minor undifferentiated	planes, vughs	coatings, nodules, infillings, excrements	plant residues
8	ice wedge cast, interior	compact grain with diagonal platy overprint	single-spaced to close porphyric	quartz, K-feldspar, plagioclase feldspar, muscovite, opaques	stipple-speckled with minor undifferentiated	planes, vughs	coatings, nodules, infillings	plant residues
8	ice wedge cast, exterior	compact grain	single-spaced to close porphyric	quartz, K-feldspar, plagioclase feldspar, muscovite, opaques	stipple-speckled with minor undifferentiated	vughs, channels	coatings, nodules, infillings	plant residues
9	buried A-horizon underlying modern C(?)	platy	single-spaced to close porphyric	quartz, K-feldspar, plagioclase feldspar, muscovite, opaques	stipple-speckled with minor undifferentiated	planes, vughs	coatings, nodules, infillings	plant residues
10	buried A/Bw-horizons	platy	single-spaced to close porphyric	quartz, K-feldspar, plagioclase feldspar, muscovite, opaques	stipple-speckled with minor undifferentiated	planes, vughs	coatings, nodules, infillings	plant residues
11	clay lens above loess, west adjacent to sample 12	platy with subangular blocky in clay lens	single-spaced to close porphyric	quartz, K-feldspar, plagioclase feldspar, muscovite, opaques	stipple-speckled with minor undifferentiated, granostratified in clay lens	planes, vughs	coatings, nodules, infillings	plant residues
12	clay lens above loess, east adjacent to sample 11	platy with subangular blocky in clay lens	single-spaced to close porphyric	quartz, K-feldspar, plagioclase feldspar, muscovite, opaques	stipple-speckled with minor undifferentiated, granostratified in clay lens	planes, vughs	coatings, nodules, infillings	plant residues
13	loess below paleosol	compact grain	single-spaced to close porphyric	quartz, K-feldspar, plagioclase feldspar, muscovite, opaques	stipple-speckled with minor undifferentiated	vughs	coatings, nodules, infillings	plant residues
14	buried A/Bw-horizons and underlying loess	compact grain with platy overprint	single-spaced to close porphyric	quartz, K-feldspar, plagioclase feldspar, muscovite, opaques	stipple-speckled with minor undifferentiated	planes, vughs	coatings, nodules, infillings	plant residues

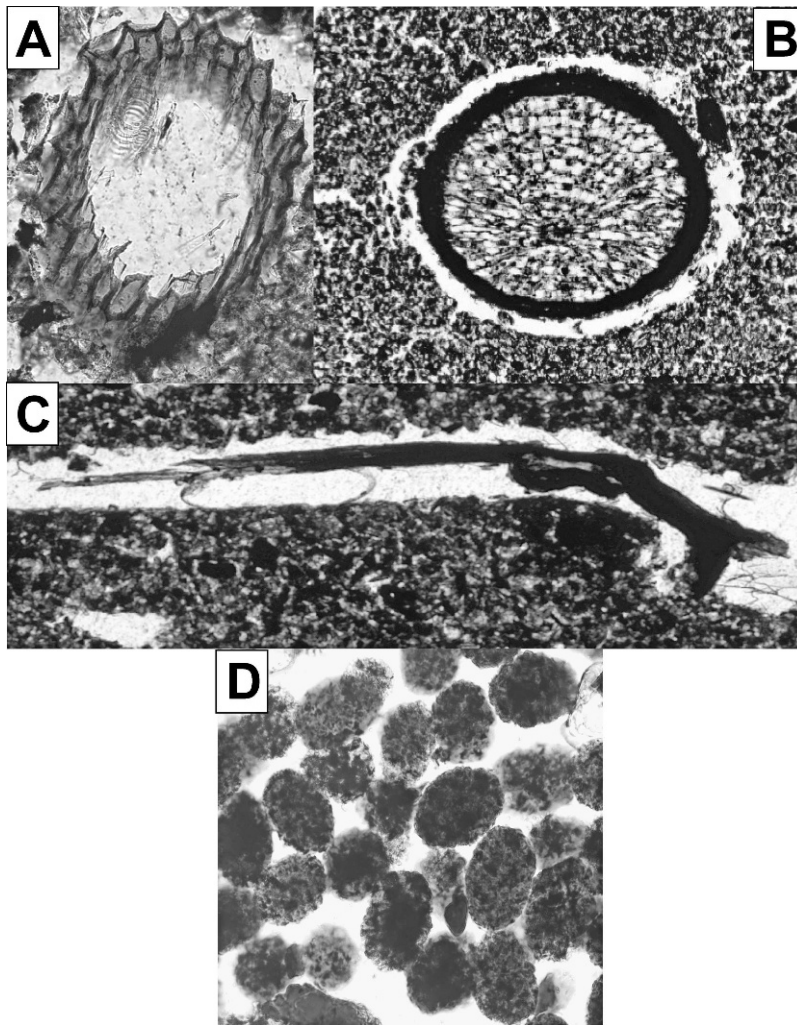


FIGURE 6. Photomicrographs of various organic remains. (A) Root cross section, ca. 0.25 mm long axis; note jagged epidermis characteristic of boreal vegetation (PPL @ 200 \times). (B) Root cross section of boreal angiosperm, ca. 0.50 mm long axis (PPL @ 100 \times). (C) Conifer needle in channel void, ca. 3.5 mm long (PPL @ 40 \times). (D) Reddish-brown ellipsoidal oribatid mite droppings; the largest are \sim 0.05 mm on the long axis (PPL @ 200 \times).

CLAY DEPOSITS

Non-pedogenic deposits of clay are present within the loess-paleosol sequence at the Chena Hot Springs Road site and were previously documented at other nearby sites (P  w  , 1975; Rieger et al., 1963). These deposits occur in the form of thin clay beds and lenses (Fig. 8). They are distinguishable microscopically by their

higher birefringence and fine subangular blocky structure. Subangular blocky microstructure can also form in cryoturbated soils and sediments. Unlike the formation of platy microstructure, subangular blocky microstructures in boreal environments are commonly formed by reticulate ice veins because the fine-grained sediments inhibit soil-water movement (Van Vliet-Lano  , 1998; Todisco and Bhiry, 2008).

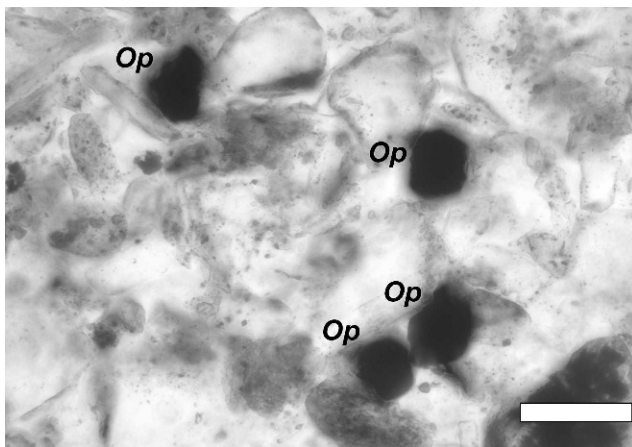


FIGURE 7. Photomicrograph (PPL[Conoscopic] @ 400 \times) from sample 13, showing typical iron-oxide grains (opaques [Op]) in loess (scale bar = 50 μ m).

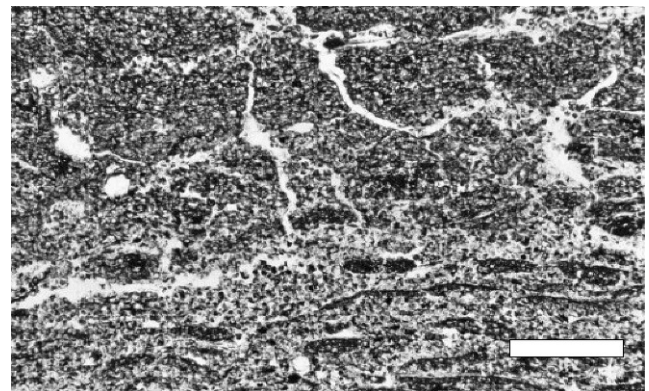


FIGURE 8. Photomicrograph (PPL @ 20 \times) from sample 11, showing clay lens above uppermost loess. Note juxtaposition of subangular blocky (upper) and platy (lower) microstructures (scale bar = 0.5 mm).

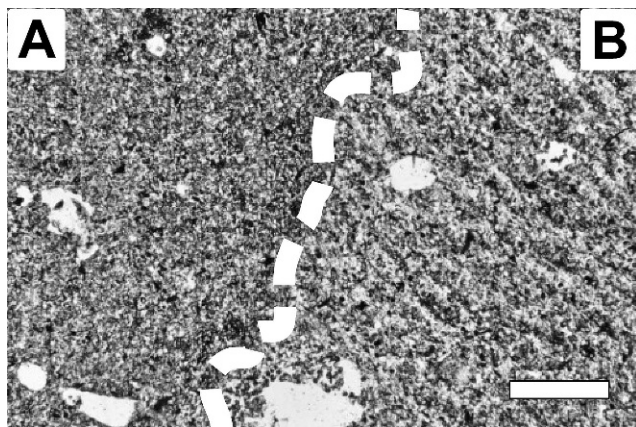


FIGURE 9. Photomicrograph (PPL @ 20 \times) from sample 8 across the lower boundary of an ice wedge cast, indicated by the dashed line. The cast fill occupies the left half of the photo (side A), while the right-half of the photo (side B) is loess into which it intruded. Note the distinct microstructural differences between the two (scale bar = 0.5 mm).

Geochemical and grain-size analyses of central Alaskan loess have shown that clay content is greater in the buried soils (6–13%) than in the surrounding loess. Also, the clay content is positively correlated with the fine silt content. Fine silt-sized particles are not known to be pedogenically produced in large quantities; therefore, relatively high amounts of both clay and fine silt within the paleosols, as compared to the unaltered loess, suggest that the clay is sedimentologic rather than pedogenic (Muhs et al., 2003). In addition, the absence of argillic (Bt) horizons in the profile, combined with little micromorphologic evidence for the illuvial transport and accumulation of clay, supports a non-pedogenic origin for the clay. Kemp (1999) and Mason et al. (2007) have previously described depositional clay crusts or lenses as rain-splash- or slopewash-related features produced by local reworking of the loess.

ICE WEDGE CAST

Sample 8 (Figs. 3 and 9) was collected across the lower boundary of an ice wedge cast. The sediments inside the cast (side A, Fig. 9) display a compact grain microstructure with a close porphyric c/f RDP (Bullock et al., 1985; Stoops, 2003). There is also much less void space in the cast fill than in the surrounding loess into which it intruded. The adjacent loess (side B, Fig. 9) has a compact grain structure with a diagonal (petrographic NW–SE) platy overprint and frequent (15–30%) void space, primarily vughs and channels (Bullock et al., 1985; Stoops, 2003). It also contains a much higher concentration of organic matter than the cast fill.

Discussion

Field and laboratory data from this and previous investigations of loess-paleosol sequences in central Alaska demonstrate that buried paleosols are a significant and paleoclimatically informative component of the loess stratigraphic record. Specifically, the paleosols indicate that loess deposition was not continuous and, at times, was sufficiently reduced so that pedogenesis could effectively operate. The depositional regimes for Alaskan and Chinese loess-paleosol sequences are considered to be quite similar in that loess deposition and pedogenesis are essentially competing processes that operate during both glacial

and interglacial periods (Begét et al., 1990; Verosub et al., 1993; Kemp and Derbyshire, 1998; Kemp, 1999).

In addition to the Chena Hot Springs Road site, Holocene loess deposition is also recorded at the Delta Junction site, approximately 130 km southeast of Fairbanks (Muhs et al., 2003). These findings confirm previously published reports of Holocene loess deposition across central Alaska (Péwé, 1975; Hamilton et al., 1983; Begét, 1990) when both loess production and accumulation rates appear to be high (Muhs et al., 2003). The presence of at least two paleosols at Delta Junction, from a section that dates to ca. 3000 ^{14}C yr B.P., evinces three episodes of loess deposition interspersed with periods of pedogenesis (Muhs et al., 2003). The accumulation of Holocene loess in central Alaska appears to be directly related to the sediment trapping ability of boreal (coniferous) vegetation, particularly spruce forests, that arrived in central Alaska between 8000 and 9000 ^{14}C yr B.P. (Ager and Brubaker, 1985; Tsoar and Pye, 1987; Muhs et al., 2003). When spruce-dominated boreal forest re-entered Alaska at the close of the last glacial period, loess accumulation rates increased dramatically. Loess deposition persists throughout central Alaska (Muhs et al., 2003).

Summary and Conclusions

Micromorphology confirmed the presence of discontinuous, weakly expressed, buried paleosols within the loess deposits at the Chena Hot Springs Road site. The soils and sediments examined in this study are early Holocene in age. Compositionally, the loess and paleosols are dominated by silt-sized quartz grains with lesser amounts of mica (muscovite variety) and feldspar (predominantly plagioclase variety). Both materials contain significant amounts of organic matter in various stages of decomposition. They exhibit microstructures that are common to soils and sediments that undergo repeated expansion and contraction, in this case from cryoturbative processes. The results of this study yielded the following conclusions:

- (1) boreal plant remains observed in all 14 thin sections support the hypothesis that Holocene loess accumulation was favored following the replacement of tundra by boreal forest;
- (2) petrography confirmed the bulk mineralogy and absence of carbonates previously documented in Fairbanks-area loesses;
- (3) the identification of detrital iron-oxide grains in all 14 thin sections is consistent with other studies of area loess that reveal high concentrations of magnetite and ilmenite, resulting in significant increases in magnetic susceptibility;
- (4) the higher clay content observed in the buried paleosols likely results from deposition during intervals of increased wind strength; and
- (5) loess deposition, which would inhibit pedogenesis, is probably related to greater wind strength, while pedogenesis, indicative of stability and minimal deposition, suggests periods of reduced wind.

Acknowledgments

I wish to thank Dr. E. Arthur Bettis III and Dr. Richard G. Baker, University of Iowa; Dr. Dan R. Muhs, U.S. Geological Survey, Denver; Dr. Brigitte Van Vliet-Lanoë, CNRS-University of Lille; Dr. Vance T. Holiday, University of Arizona; Dr. Anne E. Jennings, University of Colorado, Boulder; and two anonymous

mous reviewers for their insightful comments and valuable assistance in the preparation of this manuscript.

References Cited

- Ager, T. A., 1983: Quaternary palynology and vegetal history of Alaska. In Wright, H. E. (ed.), *Late Quaternary Environments of the United States, Volume 2: the Holocene*. Minneapolis: University of Minnesota Press, 128–141.
- Ager, T. A., and Brubaker, L., 1985: Quaternary palynology and vegetational history of Alaska. In Bryant, V. M. Jr, and Holloway, R. G. (eds.), *Pollen Records of Late-Quaternary North American Sediments*. Dallas: American Association of Stratigraphic Palynologists Foundation, 353–383.
- Begét, J. E., 1990: Middle Wisconsin climate fluctuations recorded in central Alaskan loess. *Géographie Physique et Quaternaire*, 44: 3–13.
- Begét, J. E., 2001: Continuous Late Quaternary proxy climate records from loess in Beringia. *Quaternary Science Reviews*, 20: 499–507.
- Begét, J. E., and Hawkins, D. B., 1989: Influence of orbital parameters on Pleistocene loess deposition in central Alaska. *Nature*, 337: 151–153.
- Begét, J. E., Stone, D. B., and Hawkins, D. B., 1990: Paleoclimate forcing of magnetic susceptibility variations in Alaskan loess during the Quaternary. *Geology*, 18: 40–43.
- Bettis, E. A. III, Muhs, D. R., Roberts, H. M., and Wintle, A. G., 2003: Last glacial loess in the conterminous USA. *Quaternary Science Reviews*, 22: 1907–1946.
- Birkeland, P. W., 1999: *Soils and Geomorphology*. New York: Oxford University Press, 430 pp.
- Brewer, R., 1976: *Fabric and Mineral Analysis of Soils*. Boca Raton: Robert E. Krieger, 482 pp.
- Bronger, A., and Heinkele, Th., 1989: Micromorphology and genesis of paleosols in the Luochan loess section, China: pedostratigraphical and environmental implications. *Geoderma*, 51: 167–187.
- Bullock, P., Federoff, N., Jongerius, A., Stoops, G., Tursina, T., and Babel, U., 1985: *Handbook for Soil Thin Section Description*. Albrighton, U.K.: Waine Research Publications.
- Chayes, F., 1956: *Petrographic Modal Analysis*. New York: John Wiley and Sons, 113 pp.
- Dumanski, J. A., and St. Arnaud, R. J., 1966: A micropedological study of eluviated horizons. *Canadian Journal of Earth Science*, 46: 287–292.
- Fedoroff, N., Courty, M.-A., and Thompson, M. L., 1990: Micromorphological evidence of paleoenvironmental change in Pleistocene and Holocene paleosols. In Douglas, L. A. (ed.), *Soil Micromorphology: a Basic and Applied Science*. Amsterdam: Elsevier, 653–665.
- Hamilton, T. D., 1994: Late Cenozoic glaciation of Alaska. In Plafker, G., and Berg, H. C. (eds.), *The Geology of Alaska*. Boulder: Geological Society of America, 813–844.
- Hamilton, T. D., and Brigham-Grette, J., 1991: The last interglaciation in Alaska: stratigraphy and paleoecology of potential sites. *Quaternary International*, 10–12: 49–71.
- Hamilton, T. D., Ager, T. A., and Robinson, S. W., 1983: Late Holocene ice wedges near Fairbanks, Alaska, U.S.A.: environmental setting and history of growth. *Arctic and Alpine Research*, 15: 157–168.
- Hamilton, T. D., Craig, J. L., and Sellmann, P. V., 1988: The Fox permafrost tunnel: a Late Quaternary geologic record in central Alaska. *Geological Society of America Bulletin*, 100: 948–969.
- Hovan, S. A., Rea, D. K., Pisias, N. G., and Shakelton, N. J., 1989: A direct link between the China loess and marine ^{18}O records: aeolian flux to the north Pacific. *Nature*, 340: 296–298.
- Josephs, R. L., and Bettis, E. A. III, 2003: A practical alternative to Kubiena boxes for the collection of samples for micromorphological analysis. *Geoarchaeology*, 18: 567–570.
- Josephs, R. L., and Rankin, L. K., 2008: Micromorphological investigations at the Upper Sandy Cove 3 and Porcupine Strand 23 Archaeological Sites, Labrador. *North Atlantic Archaeology*, 1: 63–76.
- Josephs, R. L., and Spiess, A. E., 2004: Micromorphological investigations at the Hedden site (4.10), a buried Paleoindian occupation along the southern Maine coast. *Current Research in the Pleistocene*, 21: 53–55.
- Kemp, R. A., 1999: Micromorphology of loess-paleosol sequences: a record of paleoenvironmental change. *Catena*, 35: 179–196.
- Kemp, R. A., and Derbyshire, E., 1998: The loess soils of China as records of climatic change. *European Journal of Soil Science*, 49: 525–539.
- Kemp, R. A., Zárate, M., Toms, P., King, M., Sanabria, J., and Arguello, G., 2006: Late Quaternary paleosols, stratigraphy and landscape evolution in the Northern Pampa, Argentina. *Quaternary Research*, 66: 119–132.
- Kukla, G., Heller, F., Ming, L. X., Chun, X. T., Sheng, L. T., and Sheng, A. Z., 1988: Pleistocene climates in China dated by magnetic susceptibility. *Geology*, 16: 811–814.
- Lagroix, F., and Banerjee, S. K., 2002: Paleowind directions from the magnetic fabric of loess profiles in central Alaska. *Earth and Planetary Science Letters*, 195: 99–112.
- Liu, T., and Ding, Z., 1998: Chinese loess and the paleomonsoon. *Annual Review of Earth and Planetary Science*, 26: 111–145.
- Maher, B. A., and Thompson, R., 1992: Paleoclimatic significance of the mineral magnetic record of the Chinese loess and paleosols. *Quaternary Research*, 37: 155–170.
- Mason, J. A., Joeckel, R. M., and Bettis, E. A. III, 2007: Middle to late Pleistocene loess record in eastern Nebraska, USA, and implications for the unique nature of Oxygen Isotope Stage 2. *Quaternary Science Reviews*, 26: 773–792.
- McDowell, P. F., and Edwards, M. E., 2001: Evidence of Quaternary climatic variations in a sequence of loess and related deposits at Birch Creek, Alaska: implications for the Stage 5 climatic chronology. *Quaternary Science Reviews*, 20: 63–76.
- Muhs, D. R., and Bettis, E. A. III, 2003: Quaternary loess-paleosol sequences as examples of climate-driven sedimentary extremes. In Chan, M. A., and Archer, A. W. (eds.), *Extreme Depositional Environments: Mega End Members in Geologic Time*. Boulder: Geological Society of America Special Paper, 370: 53–74.
- Muhs, D. R., and Budahn, J. R., 2006: Geochemical evidence for the origin of late Quaternary loess in central Alaska. *Canadian Journal of Earth Sciences*, 43: 323–337.
- Muhs, D. R., and Zárate, M., 2001: Late Quaternary eolian records of the Americas and their Paleoclimatic significance. In Markgraf, V. (ed.), *Interhemispheric Climate Linkages*. New York: Academic Press, 183–216.
- Muhs, D. R., Ager, T. A., and Begét, J., 2001: Vegetation and paleoclimate of the last interglacial period, central Alaska. *Quaternary Science Reviews*, 20: 41–61.
- Muhs, D. R., Ager, T. A., Bettis, E. A. III, McGeehin, J., Been, J. M., Begét, J. E., Pavich, M. J., Stafford, T. W. Jr, and Stevens, D. A. S. P., 2003: Stratigraphy and paleoclimatic significance of Late Quaternary loess-paleosol sequences of the last interglacial-glacial cycle in central Alaska. *Quaternary Science Reviews*, 22: 1947–1986.
- Muhs, D. R., Ager, T. A., Skipp, G., Been, J., Budahn, J., and McGeehin, J. P., 2008: Paleoclimatic significance of chemical weathering in loess-derived paleosols of subarctic central Alaska. *Arctic, Antarctic, and Alpine Research*, 40(2): 396–411.
- Mulligan, D., 2004: *Soil Survey of the Greater Fairbanks Area, Alaska*. Washington, D.C.: U.S. Department of Agriculture, 296 pp.
- Péwé, T. L., 1955: Origin of the upland silt near Fairbanks, Alaska. *Geological Society of America Bulletin*, 66: 699–724.

- Péwé, T. L., 1975: Quaternary geology of Alaska. *U.S. Geological Survey Professional Paper*, 835: 145 pp.
- Péwé, T. L., Wahrhaftig, C., and Weber, F. R., 1966: Geologic map of the Fairbanks quadrangle, Alaska. *U.S. Geological Survey Miscellaneous Investigations Map*. I-455, scale: 1:250,000.
- Péwé, T. L., Burbank, L., and Mayo, L. R., 1967: Multiple glaciations in the Yukon-Tanana Upland, Alaska. *U.S. Geological Survey Miscellaneous Investigations Map*. I-507, scale: 1:500,000.
- Rieger, S., Dement, J. A., and Sanders, D., 1963: *Soil Survey of Fairbanks Area, Alaska*. Washington D.C.: U.S. Department of Agriculture.
- Robinson, M. S., Smith, T. E., and Metz, P. A., 1990: Bedrock geology of the Fairbanks Mining District. *Alaska Division of Geological and Geophysical Surveys, Professional Report*. 106, 2 sheets, scale 1:63,360.
- Sanborn, P. T., Smith, C. A. S., Froese, D. G., Zazula, G. D., and Westgate, J. A., 2006: Full-glacial paleosols in perennially frozen loess sequences, Klondike goldfields, Yukon Territory, Canada. *Quaternary Research*, 66: 147–157.
- Stevens, T., Thomas, D. S. G., Armitage, S. J., Lunn, H. R., and Lu, H., 2007: Reinterpreting climate proxy records from late Quaternary Chinese loess: a detailed OSL investigation. *Earth Science Reviews*, 80: 111–136.
- Stoops, G., 2003: *Guidelines for Analysis and Description of Soil and Regolith Thin Sections*. Madison, Wisconsin: Soil Science Society of America, 184 pp.
- Todisco, D., and Bhiry, N., 2008: Micromorphology of periglacial sediments from the Tayara site, Qikirtaq Island, Nunavik (Canada). *Catena*, 76: 1–21.
- Tsoar, H., and Pye, K., 1987: Dust transport and the question of desert loess formation. *Sedimentology*, 34: 139–153.
- Van Vliet-Lanoë, B., 1985: Frost effects in soils. In Boardman, J. (ed.), *Soils and Quaternary Landscape Evolution*. New York: John Wiley and Sons, 117–158.
- Van Vliet-Lanoë, B., 1998: Frost and soils: implications for paleosols, paleoclimates and stratigraphy. *Catena*, 34: 157–183.
- Verosub, K. L., Fine, P., Singer, M. J., and TenPas, J., 1993: Pedogenesis and paleoclimate: interpretation of the magnetic susceptibility record of Chinese loess-paleosol sequences. *Geology*, 21: 1011–1014.
- Vlag, P. A., Oches, E. A., Banerjee, S. K., and Solheid, P. A., 1999: The paleoenvironmental-magnetic record of the Gold Hill steps loess section in central Alaska. *Physics and Chemistry of the Earth*, A24: 779–783.
- Westgate, J. A., Stemper, B. A., and Péwé, T. L., 1990: A 3 m.y. record of Pliocene–Pleistocene loess in interior Alaska. *Geology*, 18: 858–861.
- White, J. D., Koepke, B. E., and Swanson, D. K., 2002: *Soil Survey of North Star, Alaska*. Washington, D.C.: U.S. Department of Agriculture, 156 pp.
- Wright, V. P., 1986: *Paleosols: Their Recognition and Interpretation*. Princeton, New Jersey: Princeton University Press, 315 pp.
- Xiao, J., Porter, S., An, Z., Kumai, H., and Yoshikawa, S., 1995: Grain size of quartz as an indicator of winter monsoon strength on the Loess Plateau of central China during the last 130,000 yr. *Quaternary Research*, 43: 22–29.

MS accepted November 2009